
**AFRL-OSR-VA-TR-2013-0105**

# (HBCU/MI) Three-Dimensional Stable Nonorthogonal FDTD Algorithm with Adaptive Mesh Refinement for solving Maxwell's Equations

**Liu, J.**

**Delaware State University**

**March 2013**
**Final Report**



**AIR FORCE RESEARCH LABORATORY**
**AF OFFICE OF SCIENTIFIC RESEARCH (AFOSR)/RSE**
**ARLINGTON, VIRGINIA 22203**
**AIR FORCE MATERIEL COMMAND**

# REPORT DOCUMENTATION PAGE

*Form Approved*
*OMB No. 0704-0188*



**PLEASE DO NOT RETURN YOUR FORM TO THE ABOVE ORGANIZATION.**

| 1. REPORT DATE *(DD-MM-YYYY)* | 2. REPORT TYPE | 3. DATES COVERED *(From - To)* |
|---|---|---|
| 14-02-2013 | Final Performance Report | April 15, 2010 to November 14, 2012 |

**4. TITLE AND SUBTITLE**

(HBCU/MI) Three-Dimensional Stable Nonorthogonal FDTD Algorithm with Adaptive Mesh Refinement for solving Maxwell's Equations

**5a. CONTRACT NUMBER**

**5b. GRANT NUMBER**

FA9550-10-1-0127

**5c. PROGRAM ELEMENT NUMBER**

**6. AUTHOR(S)**

Liu, Jinjie

**5d. PROJECT NUMBER**

**5e. TASK NUMBER**

**5f. WORK UNIT NUMBER**

**7. PERFORMING ORGANIZATION NAME(S) AND ADDRESS(ES)**

Delaware State University
1200 N. Dupont Hwy
Dover, DE 19901

**8. PERFORMING ORGANIZATION REPORT NUMBER**

**9. SPONSORING/MONITORING AGENCY NAME(S) AND ADDRESS(ES)**

Air Force Office of Scientific Research
875 N. Randolph Street
Room 3112
Arlington, VA 22203
Dr. Arje Nachman/RSE

**10. SPONSOR/MONITOR'S ACRONYM(S)**

AFOSR

**11. SPONSOR/MONITOR'S REPORT NUMBER(S)**

**12. DISTRIBUTION/AVAILABILITY STATEMENT**

Distribution A: Approved for public release

**13. SUPPLEMENTARY NOTES**

**14. ABSTRACT**

The main objective of our effort is the development of stable, accurate and efficient Maxwell solvers. We focus on mathematical studies of the key unresolved issues in the Finite-Difference Time-Domain (FDTD) electromagnetic simulations. We have extended the subpixel smoothing FDTD method to material interface between dielectric and dispersive media by local coordinate rotation. A novel stable anisotropic FDTD algorithm based on the overlapping cells has been developed for solving Maxwell's equations of electrodynamics in anisotropic media with material interface between anisotropic dielectrics and dispersive medium or Perfect Electric Conductor (PEC). We have extended the overlapping Yee FDTD method to locally non-orthogonal grids, with application to the optical force computation on nanoparticles. We have developed a moving window full Maxwell solver algorithm with perfectly matched absorbing layer (PML) boundary conditions in order to accurately simulate the propagation of localized waves over a very long distance (millions of wavelength) in complex media. Furthermore, we have implemented the Adaptive Mesh Refine

**15. SUBJECT TERMS**

| 16. SECURITY CLASSIFICATION OF: | | | 17. LIMITATION OF ABSTRACT | 18. NUMBER OF PAGES | 19a. NAME OF RESPONSIBLE PERSON |
|---|---|---|---|---|---|
| a. REPORT | b. ABSTRACT | c. THIS PAGE | | | Jinjie Liu |
| U | U | U | U | | 19b. TELEPHONE NUMBER *(Include area code)* 302-857-7041 |

Reset

**Standard Form 298** (Rev. 8/98)
Prescribed by ANSI Std. Z39.18

## INSTRUCTIONS FOR COMPLETING SF 298

**1. REPORT DATE.** Full publication date, including day, month, if available. Must cite at least the year and be Year 2000 compliant, e.g. 30-06-1998; xx-06-1998; xx-xx-1998.

**2. REPORT TYPE.** State the type of report, such as final, technical, interim, memorandum, master's thesis, progress, quarterly, research, special, group study, etc.

**3. DATES COVERED.** Indicate the time during which the work was performed and the report was written, e.g., Jun 1997 - Jun 1998; 1-10 Jun 1996; May - Nov 1998; Nov 1998.

**4. TITLE.** Enter title and subtitle with volume number and part number, if applicable. On classified documents, enter the title classification in parentheses.

**5a. CONTRACT NUMBER.** Enter all contract numbers as they appear in the report, e.g. F33615-86-C-5169.

**5b. GRANT NUMBER.** Enter all grant numbers as they appear in the report, e.g. AFOSR-82-1234.

**5c. PROGRAM ELEMENT NUMBER.** Enter all program element numbers as they appear in the report, e.g. 61101A.

**5d. PROJECT NUMBER.** Enter all project numbers as they appear in the report, e.g. 1F665702D1257; ILIR.

**5e. TASK NUMBER.** Enter all task numbers as they appear in the report, e.g. 05; RF0330201; T4112.

**5f. WORK UNIT NUMBER.** Enter all work unit numbers as they appear in the report, e.g. 001; AFAPL30480105.

**6. AUTHOR(S).** Enter name(s) of person(s) responsible for writing the report, performing the research, or credited with the content of the report. The form of entry is the last name, first name, middle initial, and additional qualifiers separated by commas, e.g. Smith, Richard, J, Jr.

**7. PERFORMING ORGANIZATION NAME(S) AND ADDRESS(ES).** Self-explanatory.

**8. PERFORMING ORGANIZATION REPORT NUMBER.** Enter all unique alphanumeric report numbers assigned by the performing organization, e.g. BRL-1234; AFWL-TR-85-4017-Vol-21-PT-2.

**9. SPONSORING/MONITORING AGENCY NAME(S) AND ADDRESS(ES).** Enter the name and address of the organization(s) financially responsible for and monitoring the work.

**10. SPONSOR/MONITOR'S ACRONYM(S).** Enter, if available, e.g. BRL, ARDEC, NADC.

**11. SPONSOR/MONITOR'S REPORT NUMBER(S).** Enter report number as assigned by the sponsoring/ monitoring agency, if available, e.g. BRL-TR-829; -215.

**12. DISTRIBUTION/AVAILABILITY STATEMENT.** Use agency-mandated availability statements to indicate the public availability or distribution limitations of the report. If additional limitations/ restrictions or special markings are indicated, follow agency authorization procedures, e.g. RD/FRD, PROPIN, ITAR, etc. Include copyright information.

**13. SUPPLEMENTARY NOTES.** Enter information not included elsewhere such as: prepared in cooperation with; translation of; report supersedes; old edition number, etc.

**14. ABSTRACT.** A brief (approximately 200 words) factual summary of the most significant information.

**15. SUBJECT TERMS.** Key words or phrases identifying major concepts in the report.

**16. SECURITY CLASSIFICATION.** Enter security classification in accordance with security classification regulations, e.g. U, C, S, etc. If this form contains classified information, stamp classification level on the top and bottom of this page.

**17. LIMITATION OF ABSTRACT.** This block must be completed to assign a distribution limitation to the abstract. Enter UU (Unclassified Unlimited) or SAR (Same as Report). An entry in this block is necessary if the abstract is to be limited.

# AFOSR Final Performance Report

**Project Title:** (HBCU/MI) Three-Dimensional Stable Nonorthogonal FDTD Algorithm with Adaptive Mesh Refinement for solving Maxwell's Equations

**Award Number:** FA9550-10-1-0127

**Period of Performance:** April 15, 2010 – November 14, 2012

**Program Manager:** Dr. Arje Nachman

AFOSR/RSE,
875 North Randolph Road
Suite 325, Room 3112
Arlington, VA 22203
Email: Arje.nachman@afosr.af.mil
Phone: (703) 696-8427
Fax: (703) 696-8450

**Principal Investigator:** Dr. Jinjie Liu

Department of Mathematical Sciences
Delaware State University
1200 N DuPont Hwy
Dover, DE 19901
Email: jliu@desu.edu
Phone: (302) 857-7041
Fax: (302) 857-7054

**Technical Consultant:** Dr. Moysey Brio

Department of Mathematics
The University of Arizona
617 N. Santa Rita Ave
Tucson, AZ, 85721
Email: brio@math.arizona.edu
Phone: (520) 621-4582
Fax: (520) 621-8322

# 1 Accomplishments/New Findings

- We have extended the subpixel smoothing Finite-Difference Time-Domain (FDTD) method to material interface between dielectric and dispersive media by local coordinate rotation. Our method is equivalent to the previously proposed subpixel smoothing method for dielectric interface, and the extension to dispersive/dielectric interface does not require split fields so our method has improved the efficiency in comparison to the previous proposed split field approach.

- A novel stable anisotropic FDTD algorithm based on the overlapping cells has been developed for solving Maxwell's equations of electrodynamics in anisotropic media with interface between anisotropic dielectrics and dispersive medium or Perfect Electric Conductor (PEC). The previous proposed conventional anisotropic FDTD methods suffer from the late-time instability due to the extrapolation of the field components near the material interface. Our anisotropic Overlapping Yee (OY) FDTD method is stable, as it relies on the overlapping cells to provide the collocated field values without any interpolation or extrapolation. Numerical results on eigenvalue analysis confirm that our method is stable. We has applied our method to simulate the electromagnetic invisibility cloaking devices.

- We have extended our recently proposed OY FDTD method to locally non-orthogonal grids, with application to the optical force computation on nanoparticles. The subpixel-smoothing FDTD technique has successfully achieves second-order accuracy by using an inverse dielectric tensor. However, a remaining challenge is to accurately handle objects with sharp corners, where the accuracy is still less than second-order. Our approach has attained second-order convergence when sharp corners present.

- We have developed a moving window full Maxwell solver algorithm with perfectly matched absorbing layer (PML) boundary conditions in order to accurately simulate the propagation of localized waves over a very long distance (millions of wavelength) in complex media. An existing finite difference moving frame method developed more than a decade ago is inadequate due to low order transparent boundary conditions. Our method enables the realistic and predictive simulations of high intensity optical pulses in regime for which current direct Maxwell solvers are inapplicable due to memory and CPU requirements.

- We have implemented the Adaptive Mesh Refinement (AMR) FDTD method to study the ground penetrating radar devices. This work was included in the MS thesis of a graduate student.

# 2 Subpixel smoothing FDTD Maxwell solver for dielectric/dispersive interface

We have developed a new way to extend the subpixel smoothing FDTD algorithm proposed in [1, 2] to material interfaces between dielectric and dispersive media by using local coordinate rotation. The advantage of our method is the efficiency as it does not require the storage and computation of the split fields and additional equations.

The constitutive equation that converts the electric flux $\mathbf{D}$ to electric field $\mathbf{E}$ is given by

$$\mathbf{E} = \epsilon_0^{-1} \tilde{\epsilon}^{-1} \mathbf{D}, \tag{1}$$

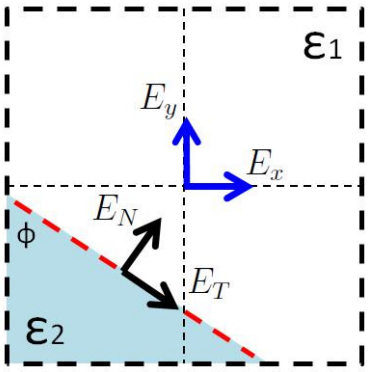


Figure 1: Electric fields near the material interface. $E_x$ and $E_y$ are the electric fields in Cartesian coordinates. $E_N$ and $E_T$ correspond to the electric fields perpendicular and tangential to the material interface respectively.

where $\epsilon_0$ is the permittivity in vacuum and $\tilde{\epsilon}^{-1}$ is the inverse permittivity tensor. Our coordinate rotation algorithm solve it in the following steps:
First, we compute the normal and tangential components of the electric fluxes $D_N$ and $D_T$ using coordinate rotation (Fig. 1)

$$\begin{pmatrix} D_N \\ D_T \end{pmatrix} = R \begin{pmatrix} D_x \\ D_y \end{pmatrix}, \tag{2}$$

where $R$ is the rotation matrix

$$R = \begin{pmatrix} \cos\phi & \sin\phi \\ \sin\phi & -\cos\phi \end{pmatrix} \tag{3}$$

Second, we compute the normal and tangential components of the electric fields $E_N$ and $E_T$ by solving the constitutive equation in the rotated coordinates.

$$\begin{pmatrix} E_N \\ E_T \end{pmatrix} = \frac{1}{\epsilon_0} \begin{pmatrix} <\epsilon^{-1}> & 0 \\ 0 & <\epsilon>^{-1} \end{pmatrix} \begin{pmatrix} D_N \\ D_T \end{pmatrix}, \tag{4}$$

where $<\cdot>$ denotes the volume average. In the rotated coordinates, the constitutive equation is a diagonal system so it is solved as two separated equations:

$$E_N = \frac{1}{\epsilon_0} <\epsilon^{-1}> D_N, \tag{5}$$

and

$$E_T = \frac{1}{\epsilon_0} <\epsilon>^{-1} D_T, \tag{6}$$

Finally, we update the elelctric fields in the regular Cartesian coordinates $E_x$ and $E_y$ using inverse rotation

$$\begin{pmatrix} E_x \\ E_y \end{pmatrix} = R^{-1} \begin{pmatrix} E_N \\ E_T \end{pmatrix}. \tag{7}$$

Combing three steps, the constitutive equation becomes

$$\begin{pmatrix} E_x \\ E_y \end{pmatrix} = \frac{1}{\epsilon_0} R^{-1} \begin{pmatrix} <\epsilon^{-1}> & 0 \\ 0 & <\epsilon>^{-1} \end{pmatrix} R \begin{pmatrix} D_x \\ D_y \end{pmatrix}. \tag{8}$$

Let $P = N^T N$ be the projection matrix where $N$ is the unit normal vector, we see that equation (8) is equivalent to equation (1) if we let

$$\tilde{\epsilon}^{-1} = P < \epsilon^{-1} > +(1 - P) < \epsilon >^{-1}, \tag{9}$$

where $\tilde{\epsilon}^{-1}$ is the inverse permittivity tensor for the subpixel smoothing algorithm [1]. Therefore, we see that the coordinate rotation results in the same formulation as the subpixel smoothing method for a dielectric interface.

To illustrate how to solve equations (5) and (6) on the material interface between dispersive and dielectric media without using split fields, we use the Lorentz dispersive model as example. As shown in Fig. 1, we assume that $\epsilon_1$ is a constant (dielectric material) and $\epsilon_2$ represents a Lorentz dispersive medium with dielectric function given by

$$\epsilon_2(\omega) = \epsilon_\infty - \frac{\alpha\omega_p^2}{\omega^2 - i\gamma\omega - \omega_p^2}. \tag{10}$$

In equation (6), we first compute volume averaged permittivity:

$$< \epsilon >= \beta\epsilon_2(\omega) + (1 - \beta)\epsilon_1, \tag{11}$$

where $\beta$ represents the ratio of the shaded area of the Fig. 1 to the whole area of the figure. After some simple calculation, we get

$$< \epsilon >= \hat{\epsilon}_\infty - \frac{\hat{\alpha}\hat{\omega}_p^2}{\omega^2 - i\hat{\gamma}\omega - \hat{\omega}_p^2}, \tag{12}$$

where $\hat{\epsilon}_\infty = \beta\epsilon_\infty + (1 - \beta)\epsilon_1$, $\hat{\alpha} = \beta\alpha$, $\hat{\omega}_p = \omega_p$, and $\hat{\gamma} = \gamma$. By introducing the polarization $P_T$, we have

$$D_T = \epsilon_0 < \epsilon > E_T = \epsilon_0(\hat{\epsilon}_\infty E_T + P_T), \tag{13}$$

where

$$P_T = -\frac{\hat{\alpha}\hat{\omega}_p^2}{\omega^2 - i\hat{\gamma}\omega - \hat{\omega}_p^2} E_T. \tag{14}$$

Equation (14) is a Lorentz model and can be solved by the Auxiliary Differential Equation (ADE) algorithm [3]:

$$\frac{\partial^2 P_T}{\partial t^2} + \hat{\gamma}\frac{\partial P_T}{\partial t} + \hat{\omega}_p^2 P_T = \hat{\alpha}\hat{\omega}_p^2 E_T. \tag{15}$$

For the normal component of the electric field in equation (5), we have the harmonic averaging

$$< \epsilon^{-1} >= \beta\frac{1}{\epsilon_2(\omega)} + (1 - \beta)\frac{1}{\epsilon_1}, \tag{16}$$

which leads to

$$\frac{1}{< \epsilon^{-1} >} = \breve{\epsilon}_\infty - \frac{\breve{\alpha}\breve{\omega}_p^2}{\omega^2 - i\omega\breve{\gamma} - \breve{\omega}_p^2}, \tag{17}$$

where $\breve{\epsilon}_\infty = \epsilon_\infty\epsilon_1/\xi$, $\breve{\alpha} = \alpha\beta\epsilon_1^2/\xi^2$, $\breve{\omega}_p^2 = \omega_p^2 + \omega_p^2(1 - \beta)\alpha/\xi$, and $\xi = \beta\epsilon_1 + (1 - \beta)\epsilon_\infty$. Similarly to the previous case, from equation (5), we get

$$D_N = \epsilon_0\frac{1}{< \epsilon^{-1} >} E_N = \epsilon_0(\breve{\epsilon}_\infty E_N + P_N), \tag{18}$$

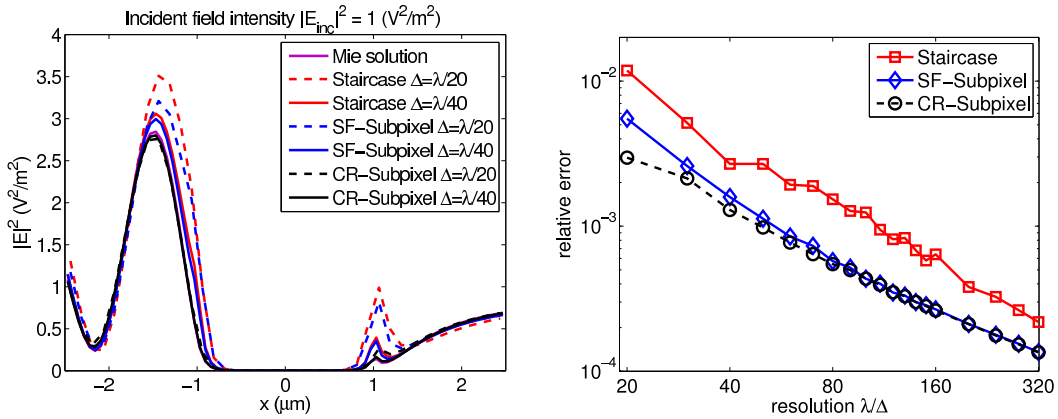


(a) (b)

Figure 2: (a) Electric fields intensity along the x-axis passing through the center of a cylinder. (b) Relative error versus resolution.

where $P_N$ is the normal component of the polarization

$$P_N = -\frac{\breve{\alpha}\breve{\omega}_p^2}{\omega^2 - i\breve{\gamma}\omega - \breve{\omega}_p^2} E_N. \tag{19}$$

Equation (19) is also a Lorentz model and can be solved in the same way as the previous case in equation (14).

The split field subpixel method proposed in [4] consider a general interface between two dispersive media. If one side of the interface is a dielectric medium, it can be reduced to two auxiliary variables since $< \epsilon^{-1} >$ in equation (9) is given in equation (17). However, split fields are still required since it cannot be further simplified, unless by using a common denominator which will result in higher order differential equations due to the higher order $\omega$ terms. In contrast, our method is a diagonal system so the constitutive equation can be solved separately and the field splitting is avoided. A limitation of our method is that it applies to the case where one side of the interface is a dispersive medium. For an interface between two dispersive media, split fields are still required. We would like to point out that the normal and tangential components of the electric fields and fluxes ($E_N$, $E_T$, $D_N$, and $D_T$) in our algorithm serve as intermediate variables, so except for a few temporary variables, no additional computational memory is required.

We test our method (the coordinate rotation (CR) subpixel smoothing) for a scattering problem and compare it with the split field (SF) subpixel smoothing method, the standard FDTD method, and the Mie solution. In our numerical simulation, a cylindrical particle with refractive index $n = 0.23 + 2.97i$ is modeled by the Lorentz model. Fig. 2 shows the electric field intensity along the x-axis passing through the center of the cylinder and the comparison of the relative error versus the resolution. The subpixel smoothing method consistently achieves smaller error in comparison to the staircased FDTD results. We also see that although our method does not achieve second order accuracy, it does significantly improve the accuracy. Table 1 shows the comparison on CPU time and memory usage for the three methods. In comparison to the SF-subpixel smoothing, our method appears to have better accuracy when the numerical grid resolution is low and it saves about 10% of memory and about 25% of CPU time.

Table 1: Comparison of CPU time and memory usage

| | $\Delta = \lambda/40$ | | $\Delta = \lambda/80$ | |
|---|---|---|---|---|
| Method | Memory | Runtime | Memory | Runtime |
| staircase | 13 MB | 7 sec | 50 Mb | 77 sec |
| CR | 21 MB | 9 sec | 85 Mb | 120 sec |
| SF | 23 MB | 12 sec | 93 Mb | 150 sec |

# 3 Overlapping Yee FDTD method for Material Interfaces between Anisotropic Dielectrics and General Dispersive or PEC Media

The anisotropic FDTD method have been studied for many years [5, 6, 7, 8, 9, 10, 11, 2, 12]. Reference [11] pointed out that for stable algorithm it is sufficient to have the finite-difference operator that converts $\mathbf{D}$ to $\mathbf{E}$ (the material matrix) to be symmetric and positive semidefinite. In the same paper, the authors developed a stable FDTD algorithm for anisotropic dielectrics and showed that the previously developed methods lead to asymmetric material matrices, which implied instability. Stability analysis in case of non-uniform dielectric was provided. The method presented in [11] only consider the case where the anisotropic dielectrics are away from the material interface. When the anisotropic dielectrics are very close to the material interface, such as the interface between dielectrics and dispersive media and between dielectrics and Perfect Electric Conductor (PEC) boundaries, extrapolation is required [7].

For anisotropic materials, the constitutive equations are given by

$$\begin{pmatrix} D_x \\ D_y \\ D_z \end{pmatrix} = \epsilon_0 \begin{pmatrix} \epsilon_{xx} & \epsilon_{xy} & \epsilon_{xz} \\ \epsilon_{yx} & \epsilon_{yy} & \epsilon_{yz} \\ \epsilon_{zx} & \epsilon_{zy} & \epsilon_{zz} \end{pmatrix} \begin{pmatrix} E_x \\ E_y \\ E_z \end{pmatrix}, \tag{20}$$

$$\begin{pmatrix} B_x \\ B_y \\ B_z \end{pmatrix} = \mu_0 \begin{pmatrix} \mu_{xx} & \mu_{xy} & \mu_{xz} \\ \mu_{yx} & \mu_{yy} & \mu_{yz} \\ \mu_{zx} & \mu_{zy} & \mu_{zz} \end{pmatrix} \begin{pmatrix} H_x \\ H_y \\ H_z \end{pmatrix}, \tag{21}$$

where matrices $\epsilon = \{\epsilon_{ij}\}$ and $\mu = \{\mu_{ij}\}$ are generally non-diagonal. In order to solve equation (20) for the electric fields $\mathbf{E}$, all components of the electric fields and fluxes need to be collocated at the same location. Similarly, for equation (21), all components of the magnetic fields must be collocated. The standard FDTD Yee lattice is staggered, so only one component of the field is provided at each location. In order to obtain the other two components, a conventional way is to average neighbor values. However, as it has been pointed out in [11], direct averaging causes late-time instability and a stable interpolation algorithm has been proposed in the same article. A limitation of the method proposed in [11] is that it considers only the case where the anisotropic dielectrics are away from the material interface. If the anisotropic dielectrics are very close to the material interface, such as the interface between dielectrics and dispersive material or PEC boundaries, extrapolation is required. We have found that the extrapolation will result in late-time instability, similar to the previous case where no material interface presents. An alternative anistropic FDTD using Finite Elements near the PEC boundaries is proposed in [12], but it is limited to PEC boundaries and does not handle problems with magnetic anisotropy.

In order to overcome this late-time instability, we propose a new stable FDTD Maxwell solver for anisotropic media, based on the idea of using overlapping cells. The usage of overlapping cells guarantees the collocation of field components so that the interpolation and extrapolation that

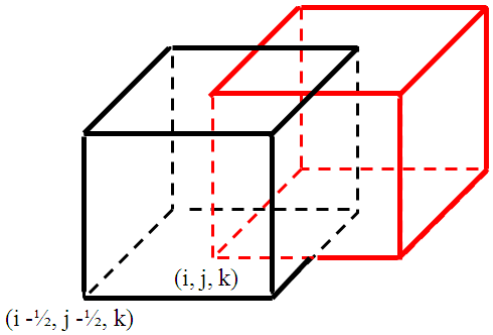


Figure 3: A 3D computational cell and its corresponding overlapping cell in x-y plane.

cause instability is avoided. This material interface could be the interface between dielectrics and dispersive medium, the interface between dielectric and PEC boundary or possibly other types of boundaries. Since the OY FDTD has the same numerical discretization as the standard Yee FDTD method (but on multiple grids), the same source conditions and perfectly matched layer (PML) boundary conditions apply.

As shown in Fig. 3, an overlapped mesh is constructed by shifting the primary grid by half cells in the x-y plane. The z-coordinates do not change. Note that in 3D, the overlapped mesh is not the dual mesh since the dual mesh is generated by shifting the grid by half cell in all three directions. Similarly, on the y-z and z-x planes, we construct two other overlapped meshes. Therefore, the 3D OY mesh contains four Yee lattices.

On each Yee grid, the standard Yee FDTD method is applied to update electric/magnetic fluxes using the information of the nearby magnetic/electric fields. After updating the fluxes, the local constitutive equations are used to solve for electric/magnetic fields. For instance, to update $\mathbf{E}$ at $(i+\frac{1}{2},j,k)$ at time step $n$, we solve the following $3\times 3$ linear system:

$$\begin{pmatrix} D_x^n(i+\frac{1}{2},j,k) \\ D_y^n(i+\frac{1}{2},j,k) \\ D_z^n(i+\frac{1}{2},j,k) \end{pmatrix} = \epsilon_0 \begin{pmatrix} \epsilon_{xx} & \epsilon_{xy} & \epsilon_{xz} \\ \epsilon_{yx} & \epsilon_{yy} & \epsilon_{yz} \\ \epsilon_{zx} & \epsilon_{zy} & \epsilon_{zz} \end{pmatrix} \begin{pmatrix} E_x^n(i+\frac{1}{2},j,k) \\ E_y^n(i+\frac{1}{2},j,k) \\ E_z^n(i+\frac{1}{2},j,k) \end{pmatrix}, \tag{22}$$

where $D_x^n(i+\frac{1}{2},j,k)$, $D_y^n(i+\frac{1}{2},j,k)$, and $D_z^n(i+\frac{1}{2},j,k)$ belong to three different Yee lattices.

We have applied our method to simulate the cylindrical cloak proposed in [13]. In the cloaking shell, the electric permittivity and magnetic permeability are functions of the radius $r$:

$$\epsilon_r(r) = \frac{r-R_1}{r}, \tag{23}$$

$$\epsilon_\theta(r) = \frac{r}{r-R_1}, \tag{24}$$

$$\mu_z(r) = \frac{r-R_1}{r}\left(\frac{R_2}{R_2-R_1}\right)^2, \tag{25}$$

where $R_2$ and $R_1$ are the radii of the outer and inner circles of the cloaking shell respectively, as shown in Fig. 4. The inner circle is a PEC shell. We consider the transverse-electric (TE) polarized electromagnetic wave propagation in $x$ direction.

In our numerical simulations, the incident wave is a plane wave propagating in x-direction with wavelength $\lambda = 0.15\ m$. The object to be cloaked is a circular cylinder with radius $R_1 = 0.1\ m$ and the cloaking shell has thickness $0.1\ m$, so $R_2 = 0.2\ m$. The computational domain is surrounded by

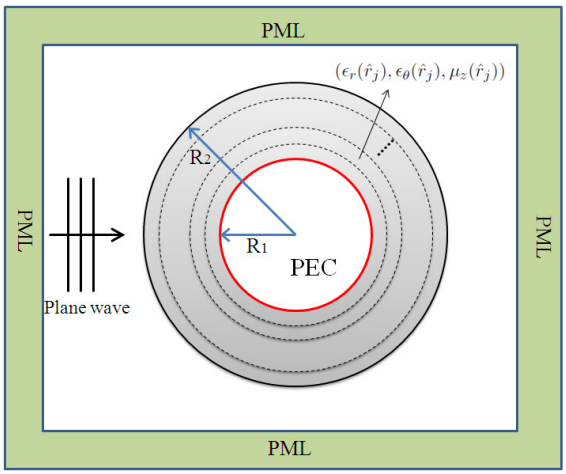


Figure 4: Computational domain for the FDTD metamaterial cloaking simulation.

PML absorbing boundaries. To avoid the singularity at $r = R_1$, the cloaking shell is approximated as a ring with eight discrete layers of homogeneous dielectric parameters, similar to [13] (Fig. 4).

We have investigated the stability of the conventional anisotropic FDTD and our OY method by computing the eigenvalues of the fully discrete problem in two dimensions. As shown in Fig. 5, the conventional anisotropic FDTD method generates a few eigenvalues outside the unit circle. As a result, the solution grows slowly and eventually blows up. In contrast, the OY method has all eigenvalues located on the unit circle which guarantees the stability.

Using the cloaking simulation, we compare the conventional anisotropic FDTD and our anisotropic OY FDTD methods. Fig. 6 shows our numerical simulation results on the electric field distribution near the cloaked objects after a few thousands of steps. Both methods give correct answer at early stage, but the conventional FDTD method results in some spikes near the inner circle of the object, which is due to the extrapolation and leads to the late-time instability. These spikes are amplified as time steps increase. Our simulations show that usually after a few tens of thousands steps (sometimes just a few thousands of steps), the solution blows up. In contrast, the new OY algorithm gives smooth and stable solution for long time simulation.

# 4 Locally non-orthogonal OY FDTD method and optical force computation

The subpixel-smoothing FDTD technique proposed in [1] achieves second-order accuracy by using an inverse dielectric tensor, and this method has been extended to anisotropic media [2], combined with a recently proposed stable FDTD scheme in anisotropic media [11]. However, a remaining challenge is to accurately handle objects with sharp corners, where the accuracy is still less than second-order [1]. Another way of eliminating staircasing is to extend the FDTD methods to globally non-orthogonal meshes [14, 15, 16, 17], but these methods suffer from the late-time instability due to the non-positive definite property of the material (projection) matrices introduced by the numerical methods. Our recently developed non-orthogonal overlapping Yee (OY) FDTD method has successfully overcomed the late-time instability problem [18].

We have further investigated the non-orthogonal OY method to model the optical force computation. Second order convergence was achieved even when sharp corner presents. The OY method requires multiple Yee grids which lead to more memory and CPU costs. To improve the efficiency,

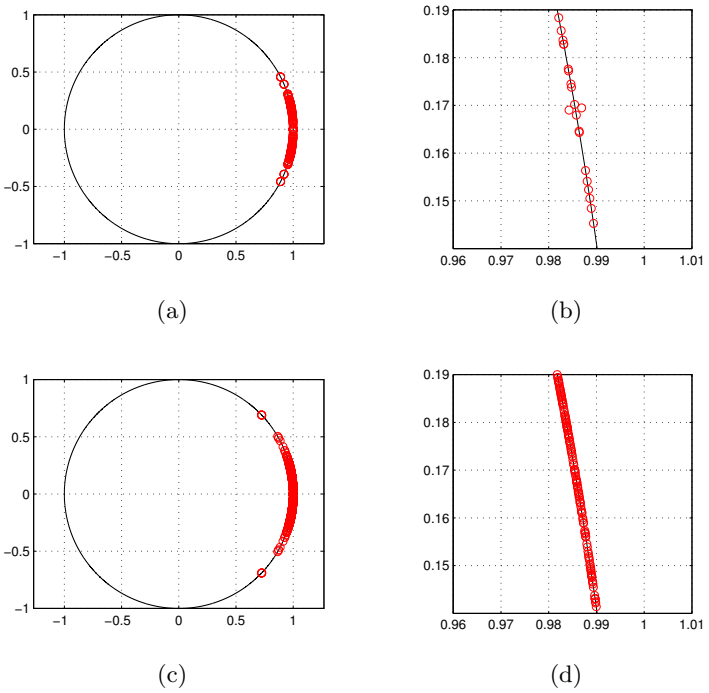


Figure 5: Distribution of the eigenvalues on the complex plane for cloaking simulation using the conventional FDTD method (upper row) and OY FDTD method (lower row). On the right are the enlarged figures.

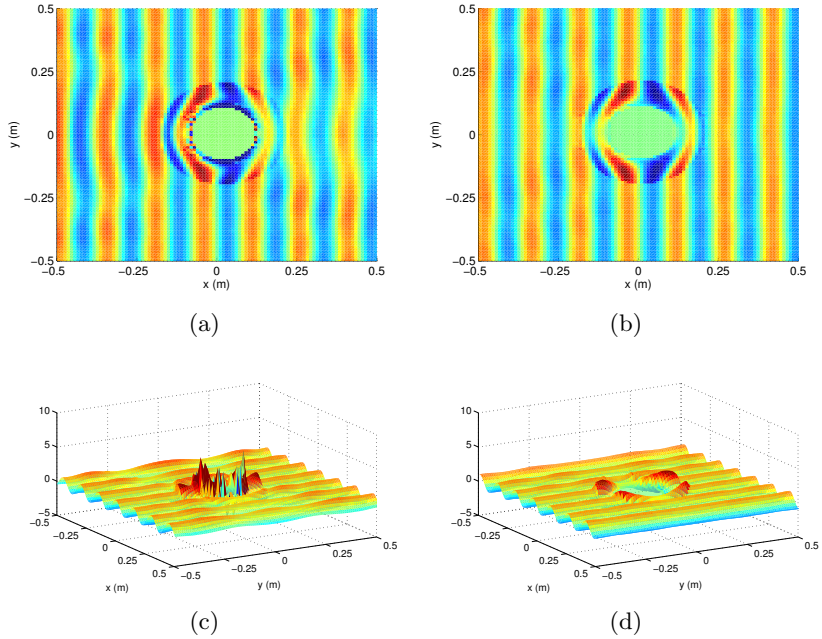


Figure 6: Numerical results on electromagnetic metamaterial cloaking simulations. Left column: the conventional anisotropic FDTD method; Right column: the anisotropic Overlapping Yee FDTD method. Upper row: contour plots of the electric field $E_y$ distribution; Lower row: surface plots of the electric field $E_y$ distribution.

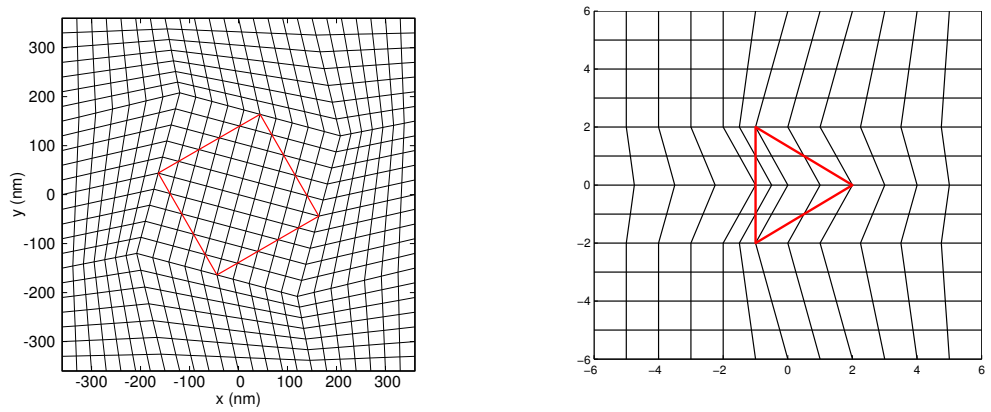


Figure 7: Non-orthogonal quadrilateral meshes near a tilted-square (Left) and triangular wedge (Right). The sides of the particles (in red) go through the diagonal vertices of the grid cells.

we propose a locally non-orthogonal OY technique. In our new implementation, the computational cells are non-orthogonal and overlapped only in a small region near the curved geometry, and the rest of the computational domain is regular Yee grid.

We use the Maxwell stress tensor formulation to compute the total optical force acting on a particle due to a time-harmonic electromagnetic field:

$$< \mathbf{F} >= \iint_S < \mathbf{T} > \cdot \, d\mathbf{S}, \tag{26}$$

where $\mathbf{T}$ is the stress tensor

$$T_{ij} = \epsilon E_i E_j + \mu H_i H_j - \frac{1}{2}(\epsilon E^2 + \mu H^2)\delta_{ij}. \tag{27}$$

The angle brackets indicate time-averaged values. $S$ is a surface that enclose the object. A simple choice of the surface $S$ is a cubic box outside the object.

The diagonal split-cell model is employed to construct quadrilateral meshes that avoids the permittivity averaging. The diagonal split-cell model has been discussed in Taflove's book [3] for orthogonal Cartesian grid. We have extended this model to non-orthogonal grids. As shown in Fig. 7, the quadrilateral mesh is constructed in such a way that the material interface does not go along cell edges but passes through the diagonal vertices of the cells using a smooth circle mapping method similar to the method proposed in [19]. Besides the simple test cases (e.g., a circular cylinder or a rectangle), our method can be applied to more complicated geometries, such as a triangular wedge, as shown in Fig. 7. By placing the magnetic fields at the cell centers and the electric fields along cell edges, this approach guarantees that no line integral of the electric field crosses the material interface so that the permittivity averaging is avoided. This approach is identified as the Split-Cell Overlapping Yee (SC-OY) method. The split-cell mesh construction and some preliminary result of computing force on cylindrical particle were presented in our previous published work [20]. The non-orthogonal quadrilateral split-cell mesh for structures with sharp corners, such as a titled-square, is shown in Fig. 7. The SC-OY method has at least two advantages: (1) it avoids permittivity averaging, so that the implementation is simplified; (2) it avoids tiny and near 180 degree angles for structures with large curvature so that the local error is smaller. A limitation of the split-cell approach is that it assumes nonmagnetic medium ($\mu$ is constant throughout the computational domain).

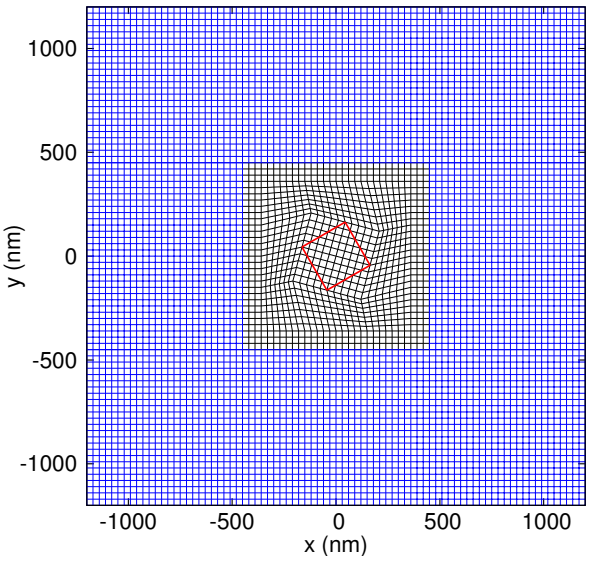


Figure 8: Locally non-orthogonal quadrilateral mesh near a tilted-square.

In general, the 2D OY technique requires two set of Yee grids to be overlapped to each other, so it doubles the computational cost. In 3D, it quadruples the cost. To improve the efficiency of OY method, we have employed a locally non-orthogonal approach. That is, in our implementation, the computational cells are only locally non-orthogonal in the region that near the curved geometry. The rest of the domain is orthogonal rectangular grids. A sample mesh is shown in Fig. 8. In the non-orthogonal region, the OY method is applied and the standard FDTD method is applied elsewhere. As shown in this figure, the non-orthogonal mesh is only about 10% of the whole computational domain, so that the overall computational cost decreases from 200% to 110%. In 3D, this locally non-orthogonal technique will further improve the performance of numerical simulation.

In our numerical examples, we have applied the nonorthogonal OY technique to compute the optical force on a tilted-square with sharp corner of 90 degrees. The side length of the square is 240 $nm$ and it is titled for 30 degrees. The incident plane wave has wavelength $\lambda = 600$ $nm$ and propagates in x-direction. The computational domain is surrounded by the uniaxial perfectly matched layer (UPML) boundaries in all directions.

Fig. 9 shows the relative errors of the computed optical forces on dielectric and metallic particles. The numerical result at very fine mesh ($\Delta = \lambda/400$) is used as the exact solution. As shown in Fig. 9, for both dielectric and metallic particles, the FDTD method converges linearly, while the OY method is second-order accuracy. For grid size $\Delta = \lambda/200$, the relative errors of the OY results are about one order of magnitude smaller than the FDTD results. Our numerical results also show that the OY solution with $\Delta = \lambda/80$ and the FDTD solution with $\Delta = \lambda/200$ have comparable errors (about 0.5%), but the OY method requires only half resource in memory usage and less than 25% resource in CPU usage.

# 5 Moving Window FDTD with PML boundaries

We have developed a novel moving window full Maxwell solver algorithm with perfectly matched absorbing layer (PML) boundary conditions in order to accuratelly simulate the propagation of localized waves over a very long distance (millions of wavelength) in complex media. Our method

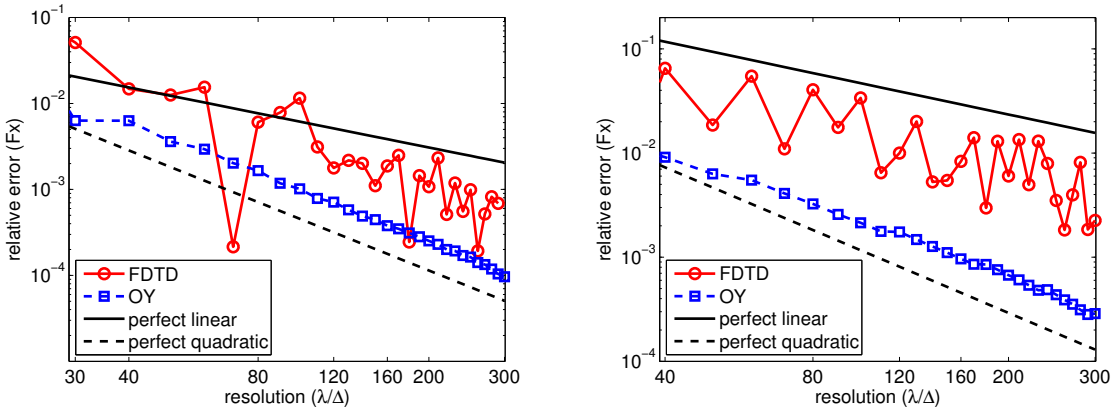


Figure 9: Relative error of forces versus resolution for tilted-square illuminated by $TE_z$ plane wave. (a) dielectric medium ($\epsilon_2 = 9$); (b) dispersive medium.

enables the realistic and predictive simulations of high intensity optical pulses in regime for which current direct Maxwell solvers are inapplicable due to memory and CPU requirements. An existing finite difference moving frame method developed more than a decade ago is inadequate due to low order transparent boundary conditions. At present, the wave propagation in a long-distance regime are modeled via asymptotically reduced unidirectional models relying on the assumption that all electromagnetic propagation modes are known and decomposition into forward-backward moving waves is possible. Both of these assumptions fail in the high contrast and nonlinear media, and for ultra-short pulses for which instantaneous frequency and amplitude become ill-defined quantities as they can change significantly within a single wave cycle.

Consider the time-domain differential form of the Maxwell equations

$$\epsilon(x,y,z)\frac{\partial}{\partial t}\mathbf{E} + \sigma(x,y,z)\mathbf{E} = \nabla\times\mathbf{H} - \mathbf{J}, \tag{28}$$

$$\mu(x,y,z)\frac{\partial}{\partial t}\mathbf{H} + \sigma^*(x,y,z)\mathbf{H} = -\nabla\times\mathbf{E}, \tag{29}$$

where material parameters $\epsilon$, $\mu$, $\sigma$, and $\sigma^*$ are the electric permittivity, magnetic permeability, electric conductivity, and magnetic conductivity, respectively. $\mathbf{J}$ is the electric current density. In inhomogeneous media, they are functions of spatial variables $x$, $y$, and $z$.

There are two ways to represent the Maxwell equations in moving frame: the Eulerian and the Lagrangian approaches. In Eulerian frame, the Maxwell equations stay the same while the material parameters are functions of space and time:

$$\epsilon(x,y,z,t)\frac{\partial}{\partial t}\mathbf{E} + \sigma(x,y,z,t)\mathbf{E} = \nabla\times\mathbf{H} - \mathbf{J}, \tag{30}$$

$$\mu(x,y,z,t)\frac{\partial}{\partial t}\mathbf{H} + \sigma^*(x,y,z,t)\mathbf{H} = -\nabla\times\mathbf{E}. \tag{31}$$

In Lagrangian frame, a transformation $x' = x - ct$ is applied where $x$ is assumed to be the direction of moving frame, so the Maxwell equations have additional advection terms:

$$\epsilon(x',y,z)\frac{\partial}{\partial t}\mathbf{E} - c\frac{\partial \mathbf{E}}{\partial x} + \sigma(x',y,z)\mathbf{E} = \nabla\times\mathbf{H} - \mathbf{J}, \tag{32}$$

$$\mu(x',y,z)\frac{\partial}{\partial t}\mathbf{H} - c\frac{\partial \mathbf{H}}{\partial x} + \sigma^*(x',y,z)\mathbf{H} = -\nabla\times\mathbf{E}. \tag{33}$$

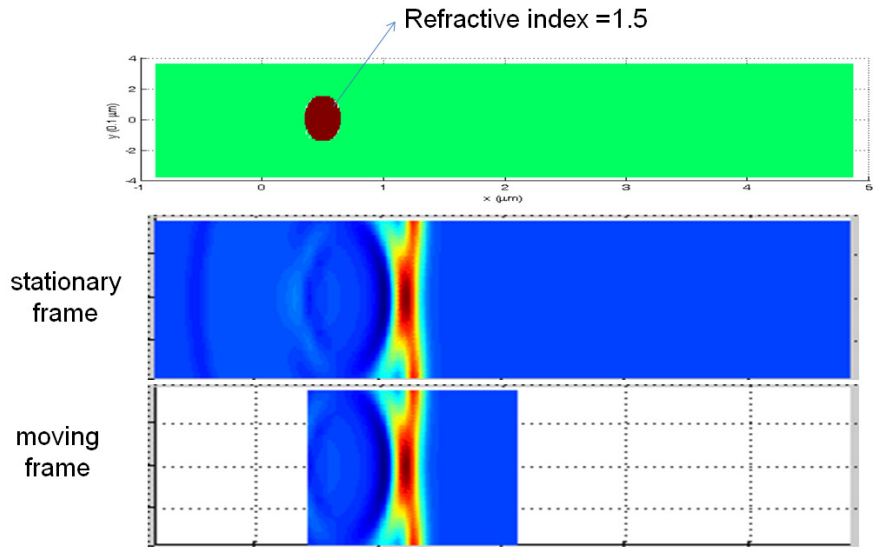


Figure 10: Simulation of optical pulse passing through a dielectric particle using stationary and moving FDTD methods.

We have studied the 2D moving window FDTD in Eulerian frame for linear media. We apply Berenger's split-field approach to implement the PML boundary conditon. Assume the moving window travels with the speed of light in $x$ direction in Eulerian frame, the split-field Maxwell equations are given by

$$\epsilon(x,y,t)\frac{\partial}{\partial t}E_x + \sigma_x(x,y,t)E_x = \frac{\partial H_z}{\partial y} - J_x, \tag{34}$$

$$\epsilon(x,y,t)\frac{\partial}{\partial t}E_y + \sigma_y(x,y,t)E_y = -\frac{\partial H_z}{\partial x} - J_y, \tag{35}$$

$$\mu(x,y,t)\frac{\partial}{\partial t}H_{zx} + \sigma_x^*(x,y,t)H_{zx} = -\frac{\partial E_y}{\partial x}, \tag{36}$$

$$\mu(x,y,t)\frac{\partial}{\partial t}H_{zy} + \sigma_y^*(x,y,t)H_{zy} = \frac{\partial E_x}{\partial y} \tag{37}$$

$$H_{zx} + H_{zy} = H_z \tag{38}$$

For Eulerian approach, the Maxwell equations are solved by the standard Yee FDTD method. The difference between the moving and the stationary FDTD method is that the time dependent material parameters need to be evaluated at every time step. Every time step, the moving window is moved by one cell toward the pulse propagation direction if the center of the main pulse has moved out of the center cell, otherwise the window is not moved. We compare our moving window FDTD results with the standard FDTD method in stationary frame. As shown in Fig. 10, good agreement between the moving and stationary FDTD is obtained for the pulse propagation through a dielectric and dispersive cylinder. The error is less than 1% after the pulse has been propagated for a relative long distance.

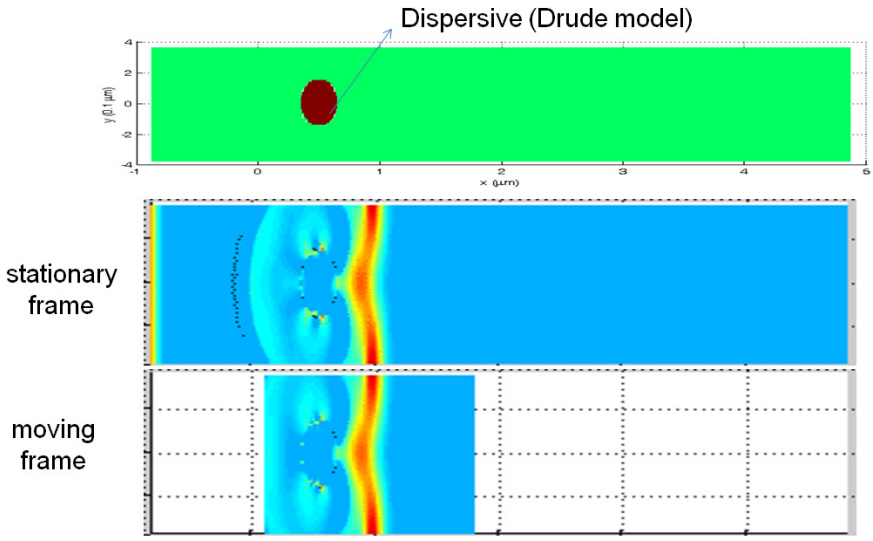


Figure 11: Simulation of optical pulse passing through a metal (dispersive) particle using stationary and moving FDTD methods.

# 6 Ground Penetrating Radar simulations by Adaptive Mesh Refinement FDTD method

The FDTD method has been applied in a wide range of applications [3, 21, 22], including antenna, microwave circuits, geophysics, optics, etc. The Ground Penetrating Radar (GPR) is a popular and efficient nondestructive electromagnetic device for high-resolution imaging of the shallow subsurface on the earth, and man-made structures. It is a technique that has been employed in many fields such as engineering, geology, and environmental studies. For example, GPR can be used to locate buried utilities and to measure snow/ice thickness. It can also be used as wall penetrating radar to 'see' through the wall. GPR systems are implemented by sending a pulse into a material via a transmitter. An integrated device records the strength and time required for the return of any reflected signals. Subsurface variations will create reflections that are picked up by the system and recorded. These reflections are produced by a variety of shapes and material, which in turn are used to form images. Under favorable conditions, GPR can provide very accurate information concerning the nature of various subsurfaces and buried objects.

We have applied the Adaptive Mesh Refinement (AMR) FDTD method to the GPR system. The AMR method allows the simulation of very small object with fine mesh inside a large region with coarse mesh. Let $E^n_{z,c}$ and $E^n_{z,f}$ denote the field values defined on coarse and fine meshes, respectively. The AMR FDTD algorithm updating the Maxwell equations in the following steps:

1. Update $E^{n+1}_{z,c}$ by $\Delta t$ from $E^n_{z,c}$.

2. Update $E^{n+\frac{1}{2}}_{z,f}$ in the interior of the fine mesh by $\frac{\Delta t}{2}$ from $E^n_{z,f}$.

3. Compute $E^{n+\frac{1}{2}}_{z,f}$ on coarse/fine boundary through interpolation of neighboring coarse mesh $E^n_{z,c}$ and $E^{n+1}_{z,c}$ electric field values.

4. Update $H^{n+\frac{3}{4}}_{x,f}$ and $H^{n+\frac{3}{4}}_{y,f}$ everywhere on the fine mesh by $\frac{\Delta t}{2}$ from $H^{n+\frac{1}{4}}_{x,f}$ and $H^{n+\frac{1}{4}}_{y,f}$ respec-

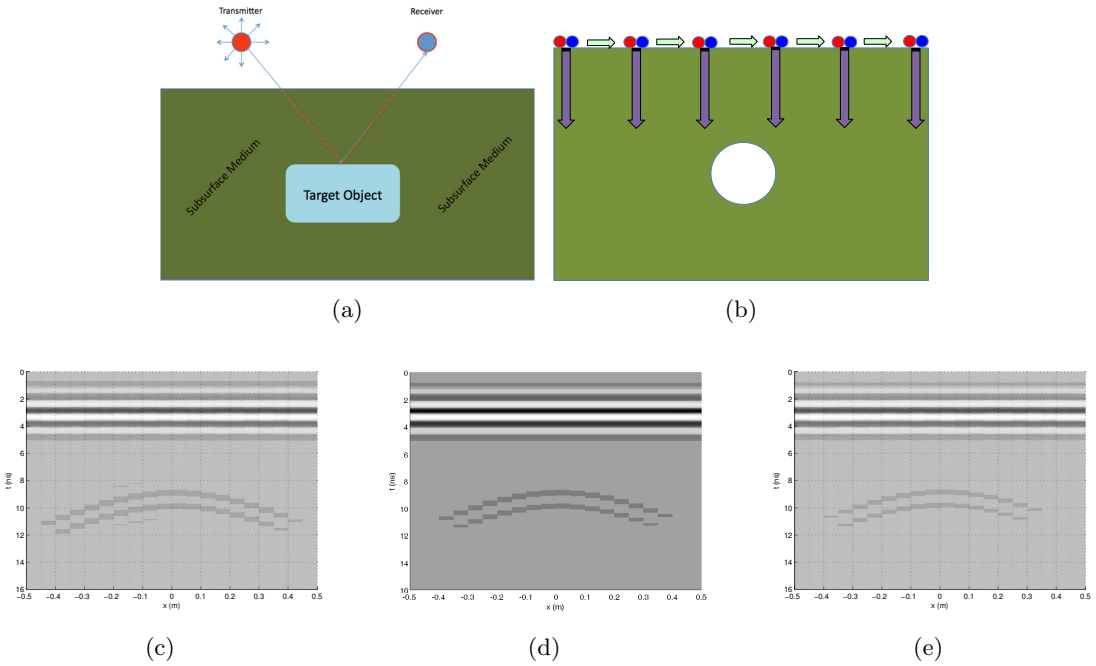


Figure 12: FDTD simulation of GPR. (a) The red and blue circles are the transmitter and receiver respectively. (b) A pulse is emitted at multiple locations along the ground and the data from reflected waves from underground object are recorded. (c): FDTD result with coarse mesh size $\Delta$ everywhere. (d): FDTD result with fine mesh size $\Delta/2$ everywhere. (e): AMR-FDTD result with fine mesh size $\Delta/2$ near the object and coarse mesh size $\Delta$ elsewhere.

tively.

5. Compute $H_{x,c}^{n+\frac{1}{2}}$ and $H_{y,c}^{n+\frac{1}{2}}$ through interpolation of neighboring fine mesh $H_{x,f}^{n+\frac{1}{4}}$, $H_{x,f}^{n+\frac{3}{4}}$, $H_{y,f}^{n+\frac{1}{4}}$ and $H_{y,f}^{n+\frac{3}{4}}$ magnetic field values.

6. Update $E_{z,f}^{n+1}$ in the interior of the fine mesh by $\frac{\Delta t}{2}$ from $E_{z,f}^{n+\frac{1}{2}}$.

7. Compute $E_{z,f}^{n+1}$ on coarse/fine boundary through interpolation of neighboring coarse mesh $E_{z,c}^{n+1}$ electric field values.

8. Update $H_{x,f}^{n+\frac{5}{4}}$ and $H_{y,f}^{n+\frac{5}{4}}$ everywhere on the fine mesh from $H_{x,f}^{n+\frac{3}{4}}$ and $H_{y,f}^{n+\frac{3}{4}}$ respectively.

9. Compute $E_{z,c}^{n+1}$ through interpolation of neighboring fine mesh $E_{z,f}^{n+1}$ field values.

10. Update $H_{x,c}^{n+\frac{3}{2}}$ and $H_{y,c}^{n+\frac{3}{2}}$ by $\Delta t$ from $H_{x,c}^{n+\frac{1}{2}}$ and $H_{y,c}^{n+\frac{1}{2}}$.

The GPR simulation set up and results are shown in Fig. 12. We compare the results of the standard and the AMR FDTD methods. For AMR simulation, the mesh is refined in a small region near the circular object. For standard FDTD simulations, the fine mesh result is much clearer than that of the coarse mesh. In the refined region, the AMR result is very similar to that of the fine mesh FDTD result, but the simulation takes much less memory and CPU time. Therefore, our AMR FDTD solver provides an efficient tool in GPR simulation.

# 7 Conclusion and future work

The main objective of this effort is the development of stable, accurate and efficient Maxwell solvers. The proposed activities focus on mathematical studies of the key unresolved issues in the Finite-Difference Time-Domain (FDTD) electromagnetic simulations. In summary, our main achievements and discovers are listed below.

- A new way of extending the subpixel smoothing FDTD algorithm to dielectric/dispersive material interface was invented by using local coordinate rotation. As our method does require split fields, better efficiency has been achieved in comparison to the previous work.
- A novel stable anisotropic overlapping Yee FDTD Maxwell solver was proposed for problem involving complex material interface, such as the electromagnetic invisibility cloaking devices. Previous proposed conventional anisotropic FDTD method suffers from the late-time instability problem in such cases due to the extrapolation near the material interface. In contrast, our method relies on the overlapping cells to provide the collocated field values without any interpolation or extrapolation.
- A locally non-orthogonal OY FDTD algorithm was developed to compute optical forces on nanoparticles. Together with diagonal split cell mesh, the OY approach attains second-order convergence for structures with smooth curved surface and with sharp corners.
- A moving window FDTD method with PML boundaries has been deveolped to model high intensity optical pulse propagation over long distance (millions of wavelength). The algorithm is based on the Eulerian formulation. Numerial tests show that the moving window method is accurate in comparison to the stationary FDTD method.
- Adaptive Mesh Refinement FDTD method has been applied to study the ground penetrating radar devices. This work was included in the MS thesis of a graduate student.

In the future, we will continue our investigation on new algorithms in numerical solutions to Maxwell's equations with applications to linear and nonlinear optics, photonics, EM theory, and metamaterials.

# References


[1] A. Farjadpour, D. Roundy, A. Rodriguez, M. Ibanescu, P. Bermel, J. D. Joannopoulos, S. G. Johnson, and G. W. Burr. Improving accuracy by subpixel smoothing in the finite-difference time domain. *Opt. Lett.*, 31(20):2972–2974, 2006.

[2] Ardavan F. Oskooi, Chris Kottke, and Steven G. Johnson. Accurate finite-difference time-domain simulation of anisotropic media by subpixel smoothing. *Opt. Lett.*, 34(18):2778–2780, 2009.

[3] A. Taflove and S. Hagness. *Computational Electrodynamics: The Finite-Difference Time-Domain Method*. Artech House, Norwood, MA, 3rd edition, 2005.

[4] A. Deinega and I. Valuev. Subpixel smoothing for conductive and dispersive media in the finite-difference time-domain method. *Opt. Lett.*, 32(23):3429–3431, 2007.

[5] J. Schneider and S. Hudson. The finite-difference time-domain method applied to anisotropic material. *IEEE Trans. Antennas Propag.*, 41:994–999, 1993.

[6] S. G. Garcia, T. M. Hung-Bao, R. G. Martin, and B. G. Olmedo. On the application of finite methods in time domain to anisotropic dielectric waveguides. *IEEE Trans. Microw. Theory Tech.*, 44:2195–2206, 1996.

[7] A. P. Zhao, J. Juntunen, and A. V. Räisänen. An efficient FDTD algorithm for the analysis of microstrip patch antennas printed on a general anisotropic dielectric substrate. *IEEE Trans. Microw. Theory Tech.*, 47(7):1142–1146, 1999.

[8] H. Mosallaei and K. Sarabandi. Magneto-dielectrics in electromagnetics: Concept and applications. *IEEE Trans. Antennas Propag.*, 52:1558–1567, 2004.

[9] L. Dou and A. R. Sebak. 3D FDTD method for arbitrary anisotropic materials. *Microw. Opt. Technol. Lett.*, 48(10):2083–2090, 2006.

[10] H. O. Lee and F. L. Teixeira. Cylindrical fdtd analysis of LWD tools through anisotropic dipping-layered earth media. *IEEE Trans. Geosci. Remote Sens.*, 45(2):383–388, 2007.

[11] Gregory R. Werner and John R. Cary. A stable FDTD algorithm for non-diagonal, anisotropic dielectrics. *J. Comput. Phys.*, 226:1085–1101, 2007.

[12] C. Kung and R. Lee. Alternative FDTD updating schemes for anisotropic materials. *IEEE Trans. Antennas Propag.*, 57(12):3903–3910, 2009.

[13] S. A. Cummer, D. Schurig B.-I. Popa, D. R. Smith, and J. B. Pendry. Full-wave simulation of electromagnetic cloaking structures. *Phys. Rev. E*, 74:036621, 2006.

[14] R. Holland. Finite-difference solution of Maxwell's equations in generalized nonorthogonal coordinates. *IEEE Trans. Nuclear Science*, NS-30:4589–4591, 1983.

[15] J.-F. Lee, R. Palandech, and R. Mittra. Modeling three-dimensional discontinuities in waveguide using nonorthogonal FDTD algorithm. *IEEE Trans. Microw. Theory Tech.*, 40(2):346–352, February 1992.

[16] N. Madsen. Divergence preserving discrete surface integral methods for Maxwell's curl equations using non-orthogonal unstructured grids. *J. Comput. Phys.*, 119:34–45, 1995.

[17] S. Gedney, F. Lansing, and D. Rascoe. Full wave analysis of microwave monolithic circuit devices using a generalized Yee-algorithm based on an unstructured grid. *IEEE Trans. Microw. Theory Tech.*, 44(2):1393–1400, 1996.

[18] J. Liu, M. Brio, and J. V. Moloney. Overlapping Yee FDTD method on nonorthogonal grids. *J. Sci. Comput.*, 39(1):129–143, 2009.

[19] D. A. Calhoun, C. Helzel, and R. J. LeVeque. Logically rectangular grids and finite volume methods for PDEs in circular and spherical domains. *SIAM Rev.*, 50(4):723–752, 2008.

[20] J. Liu, M. Brio, and J. V. Moloney. A diagonal split-cell model for the overlapping Yee FDTD method. *Acta Mathematica Scientia*, 29(6):1670–1676, 2009.

[21] Fernando L. Teixeira. Time-domain finite-difference and finite-element methods for maxwell equations in complex media. *IEEE Trans. Antennas Propag.*, 56:2150–2166, 2008.

[22] A. Taflove. A perspective on the 40-year history of FDTD computational electrodynamics. *J. Applied Computational Electromagn. Soc.*, 22:1–21, 2007.

## Personnel:

Faculty:
Dr. Jinjie Liu (PI, Delaware State University)
Dr. Moysey Brio (Technical Consultant, University of Arizona)

Graduate Students:
Mr. Pengrui Hui (Delaware State);
Ms. Yingxue Zhao (Delaware State);
Mr. Matthew Moore (Delaware State);
Mr. Penglong Xu (Delaware State);
Mr. Adonis Ajayi (Delaware State).

## Archival publications during reporting period, April 2010 - Nov. 2012:

1. J. Liu, M. Brio, and J. V. Moloney, "Subpixel smoothing Finite-Difference Time-Domain method for material interface between dielectric and dispersive media". *Optics Letters*, 37, 4802-4804, 2012.

2. J. Liu, M. Brio, and J. V. Moloney, "Computation of optical force on nanoparticles using locally non-orthogonal overlapping Yee FDTD method". *Journal of Electromagnetic Analysis and Applications*, 4, 452-456, 2012.

3. J. Liu, M. Brio, and J. V. Moloney, "An Overlapping Yee FDTD method for Material Interfaces between Anisotropic Dielectrics and General Dispersive or PEC Media". *International Journal of Numerical Modelling: Electronic Networks, Devices and Fields*, accepted December 3, 2012, in press.

4. A. Marcano, I. Basaldua, A. Villette, R. Edziah, J. Liu, O. Ziane, and N. Melikechi, "Photothermal lens spectrometry measurements in highly turbid samples", submitted to *Applied Spectroscopy*.

5. J. Liu, P. Hui, M. Brio, J. V. Moloney, "Moving window FDTD method with Perfectly Matched Layer boundaries", preprint, to be submitted.

## Interactions/Presentations:

1. Jinjie Liu, "Stable FDTD Methods for Material Interfaces", AMR western sectional meeting, University of Arizona, October 27, 2012. (Invited talk).

2. Jinjie Liu, "Subpixel Smoothing FDTD for Dielectric/Dispersive Material Interfaces", AFOSR Nonlinear Optics Meeting, Albuquerque, NM, September 18-19, 2012. (Poster).

3. Brandon Dogan and Jinjie Liu, "Finite-Difference Time-Domain simulations of Super-scattering", 2012 Delaware State University summer research symposium, July 26, 2012. (Poster).

4. Jinjie Liu, "FDTD Techniques on Overlapping Cells and Moving Meshes", International Conference on Applied Mathematics, City University of Hong Kong, Hong Kong, May 31, 2012. (Invited talk).

5. Jinjie Liu, "FDTD Techniques on Overlapping Cells and Moving Meshes", Midwest Numerical Analysis Days 2012, Univ. of Notre Dame, May 13, 2012. (Invited talk).

6. Adonis Ajayi, 'Nonuniform and Adaptive Mesh Refinement FDTD methods for Ground Penetrating Radar simulations", department of mathematical sciences, Delaware State university, November 14, 2012. (Seminar)

7. Adonis Ajayi, "Ground Penetrating Radar Simulation via the Finite-Difference Time-Domain", 2012 Delaware State University graduate research symposium, April 15, 2012. (Poster).

8. Pengrui Hui, "Moving window FDTD method with PML boundaries", 2012 Delaware State University graduate research symposium, April 15, 2012.

9. Jinjie Liu, "Overlapping Yee and Moving Frame FDTD methods", department of mathematical sciences, Delaware State university, October 25, 2011. (Seminar)

10. Jinjie Liu, "Stable Hybrid Overlapping Yee FDTD Method in Steady and Moving Frame", AFOSR Nonlinear Optics Meeting, Albuquerque, NM, Oct., 19, 2011.

11. Dorian Foster and Jinjie Liu, "Stable FDTD Simulations of Electromagnetic Cloaking Structures", 2011 Delaware State University summer research symposium, July 28, 2011. (Poster).

12. Jinjie Liu, "Generalization of the FDTD Technique to Nonorthogonal Grids and Nonlinear Media", Dept. of Mathematics and Statistics, Wichita State University, Wichita, Kansas, Mar. 11, 2011. (Invited seminar talk).

13. Jinjie Liu, "Generalization of the FDTD Maxwell solver to Nonorthogonal grids and to Nonlinear Drude Media", department of mathematical sciences, Delaware State university, February 22, 2011. (Seminar)

14. Jinjie Liu, "Stable Nonorthogonal FDTD Algorithm and the Generalization of the FDTD Method to Nonlinear Drude Media", AFOSR Nonlinear Optics Meeting, Albuquerque, NM, September 23, 2010.

## Honors/Awards:

- "Spotlight on Optics" highlights our research: Our paper "Subpixel smoothing Finite-Difference Time-Domain method for material interface between dielectric and dispersive media", published in Optics Letters in 2012, has been highlighted in "Spotlight on Optics" (December 2012): http://www.opticsinfobase.org/spotlight/summary.cfm?uri=ol-37-22-4802

- Adonis Ajayi won the first place award (MS in science area) for his poster presentation at the 2012 Delaware State University Graduate Research Symposium, April 15, 2012.

## Changes in research objectives, if any:

None

## Change in AFOSR program manager, if any:

None

## Extensions granted or milestones slipped, if any:

None

## Include any new discoveries, inventions, or patent disclosures during this reporting period (if none, report none):

None